Available online at www.sciencedirect.com

ScienceDirect

Energy Procedia 101 (2016) 750 – 757

Energy Procedia

71st Conference of the Italian Thermal Machines Engineering Association, ATI2016, 14-16 September 2016, Turin, Italy

Different Numerical Approaches for the Analysis of a Single Screw Expander

Alessio Suman[a,*], Davide Ziviani[b], Jacopo Gabrielloni[a], Michele Pinelli[a], Michel De Paepe[b], Martijn Van Den Broek[b]

[a]Engineering Department in Ferrara, University of Ferrara, Ferrara, Italy
[b]Ghent University, Department of Flow, Heat and Combustion Mechanics, Ghent, Belgium

Abstract

Positive displacement machines (e.g. scroll, twin screw, reciprocating, etc.) are proven to be suitable as expanders for organic Rankine cycle (ORC) applications, especially in the medium to low power range. However, in order to increase their performance, detailed simulation models are required to optimize the design and reduce the internal losses. In recent years, computational fluid dynamics (CFD) has been applied for the design and analysis of positive displacement machines (both compressors and expanders) with numerous challenges due to the dynamics of the expansion (or compression) process and deforming working chambers. The majority of the studies reported in literature focused on scroll, twin screw and reciprocating machines. Furthermore, the limitation of such methodologies to be applied directly to complex multi-rotor machines has been highlighted in literature.

In this paper, a single screw expander (SSE) is used as benchmark to evaluate the applicability of different grid generation methodologies (dynamic remeshing and Chimera strategy overlapping grid), in terms of computational resources required, accuracy of the results and limitations. Although, the low-order models have been applied to single screw machines, there is still a lack of CFD analyses due to the particular complexity of the machine geometry and of its working principle. The calculations have been performed with air to reduce the complexity of the problem. to the main results are two folds: (i) the assessment of a numerical strategy with respect to the most critical parameters of a dynamic mesh-based simulation and (ii) the comparison of the pressure field and internal flow features obtained by using different numerical approaches.

Peer-review under responsibility of the Scientific Committee of ATI 2016.

* Corresponding author. Tel.: +39-0532-974964.
E-mail address: alessio.suman@unife.it

Peer-review under responsibility of the Scientific Committee of ATI 2016.
doi:10.1016/j.egypro.2016.11.095

Keywords: single screw expander; CFD; dynamic mesh; overset grid; mesh morphing

1. Introduction

Organic Rankine Cycle (ORC) is a well-known technology to convert waste heat from several sources and in a wide range of power outputs [1]. Especially in the medium to low power range, volumetric expanders play an important role because of their performance and lower investment costs compared to dynamic expanders [2]. Different types of positive displacement machines, such as scroll or twin screw, have been investigated for their use in ORCs. Recently the single screw expander (SSE) is gaining interest as a potential volumetric expander for ORC applications. In comparison with the twin screw, the SSE has longer bearings life due to balanced loading on the main rotor, high volumetric efficiency, low leakage, low noise and vibration and a simplified configuration [3]. To the Author best knowledge, CFD analyses applied to single screw machines are rare due to the complexity of the problem especially regarding the mesh generation.

The aim of this paper is to evaluate and compare different meshing techniques and solution schemes when applied to a single screw geometry. Pros and cons of commercial software are discussed and the accuracy of the results is analyzed by comparing the results obtained with each of them. Both steady-state and transient analyses have been investigated. Each simulation approach can provide different insights and useful information. The steady-state simulation allows to evaluate the volumetric efficiency, axial thrusts and therefore a preliminary structural analysis. Moreover, with the steady-state approach it is possible to calculate the flow coefficients (C_d) of the gaps which relate the flow rate through the machine and the pressure drop across the gaps. This is very useful to tune lumped parameter models, where gap flow coefficients are fundamental to improve the model accuracy on the mass flow predictions [4]. At the same time, they are very difficult to be estimated by means of experimental data and/or analytical/empirical relations. For these reasons, CFD models (even steady-state) are increasingly used to determine these crucial coefficients. However, insights on the internal dynamics of the expansion process, pressure and mass flow rate fluctuations can be obtained only by means of a transient simulation [5 – 7].

Similarly to a twin screw expander, the single screw is generated by two meshing profiles: a grooved central rotor engages with the lateral toothed satellites (or gaterotors). The meshing between each groove with the corresponding tooth isolates a working chamber, i.e. a portion of the groove. The details of the main dimensions of the present SSE are listed in [8]. The real geometry (11 kWe air-compressor adapted to be an expander) has been simplified accordingly in order to perform CFD analyses. In particular, the main rotor shaft and the its sealing have been removed as well as the bearings. Similar modifications have been applied to the starwheels. The 3D CAD geometry is shown in Fig. 1.

Nomenclature

Q	Volumetric flow rate
m	Mass flow rate
ρ	Density
Δp	Pressure drop
A	Passage area
SSE	Single-screw expander
DM	Dynamic Mesh
CS	Chimera strategy
MM	Mesh morphing
SCORG	Screw compressor rotor grid generator

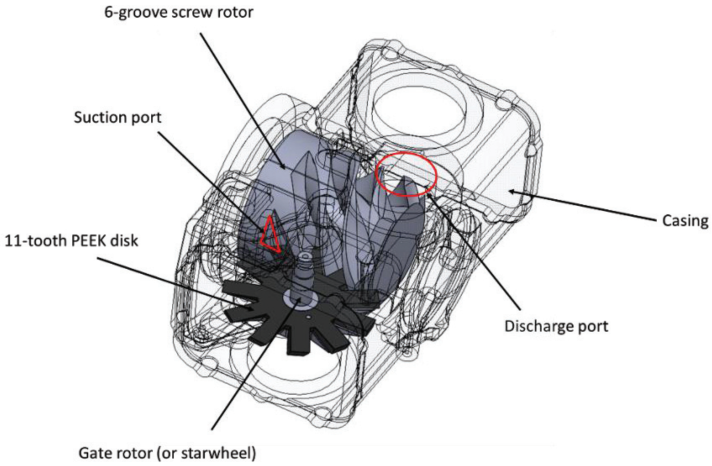

Fig. 1. Single screw expander geometry (Adapted from Ziviani et al. [9]).

2. Meshing techniques

Three different meshing techniques have been applied to the single screw expander and a comparison is proposed in the present work. Since the analyzed methodologies are not available within a single software, each technique is associated to a specific software :

- Dynamic Mesh (DM): ANSYS Fluent (v13.0);
- Chimera Strategy (CS): CD-ADAPCO STAR-CCM+ (v10.02);
- Mesh Morphing (MM): PumpLinx (v4.0.3).

2.1. Dynamic mesh

By employing the DM strategy available in ANSYS Fluent 13.0, the mesh of the fluid domain between the screw rotor and satellites is regenerated at each time step in order to follow the shape and size change of the working chamber. A transient analysis is able to reproduce the real operation of the machine through a sequence of relative positions between the central screw and the satellites by imposing an angular increment. The mesh regeneration process can be based upon element size criteria and/or element quality criteria (such as skewness). The numerical domain of the single screw expander is discretized by means of a tetrahedral mesh. To increase the resolution of the mesh close to the walls, a local mesh refining approach has to be adopted. Figure 2 highlights the grid deformations according to four subsequently time step. To be noted is that, (i) the mesh deformation from the first step (I) to the second step (II) and from the third (III) step to the fourth step (IV), and (ii) the mesh regeneration from the second step (II) to the third step (III).

2.2. Chimera strategy

Overlapping grid, subsequently named the Chimera approach, was first introduced in the early 1980's [10] when several grid assembly packages have become available [11]. The overset method consist in the contemporary use of active cells and passive cells. In active cells, regular discretized equations are solved, while in passive cells, no equation is solved, they are temporarily or permanently de-activated. Active cells along interface to passive cells refer to donor cells at another grid instead of the passive neighbors on the same grid. The first layer of passive cells next to active cells are called acceptor cells. The solution is computed on all grids simultaneously. Grids are implicitly coupled through the linear equation system matrix. Different interpolation functions can be used to express values at acceptor cells via values at donor cells. The donor cells must be active cells, and the change of cell

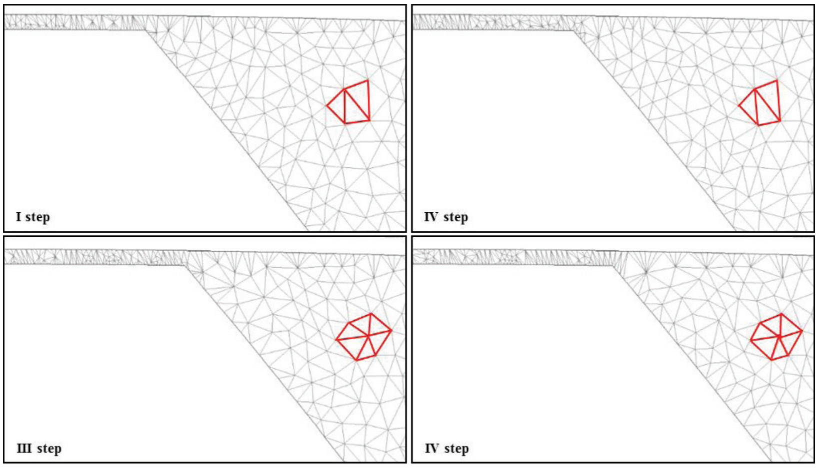

Fig. 2. Dynamic tetrahedral mesh evolution through time: mesh deformation and mesh regeneration.

status is automatically controlled by the solver. Overset grids usually involve one background mesh, which is adapted to environment, and one or more overset grids attached to bodies, overlapping the background mesh and/or each other. Each grid (background and overset) can move according to the motion models implemented in the CFD software. The major difference with respect to the DM approach consists that CS does not deform the mesh during the calculation.

In the present paper the background mesh and the three overlapping mesh are reported in Fig. 3. In this case, each overlapping grid has to interface with the background mesh, moreover there are two additional overset interfaces between each satellite and the central screw. For this particular configuration, the central screw is considered as the background for the two satellites. To obtain a good interface quality, local refinements have been done in the background mesh to lower cell dimensions in the overlapping zone and reasonably increase the element number.

Overlapping meshes are made of 5,033,265 elements (839,113 for the screw and 2,097,068 for each satellite), while the background mesh consists of 3,210,621 elements. Overlapping and background mesh are constitute by

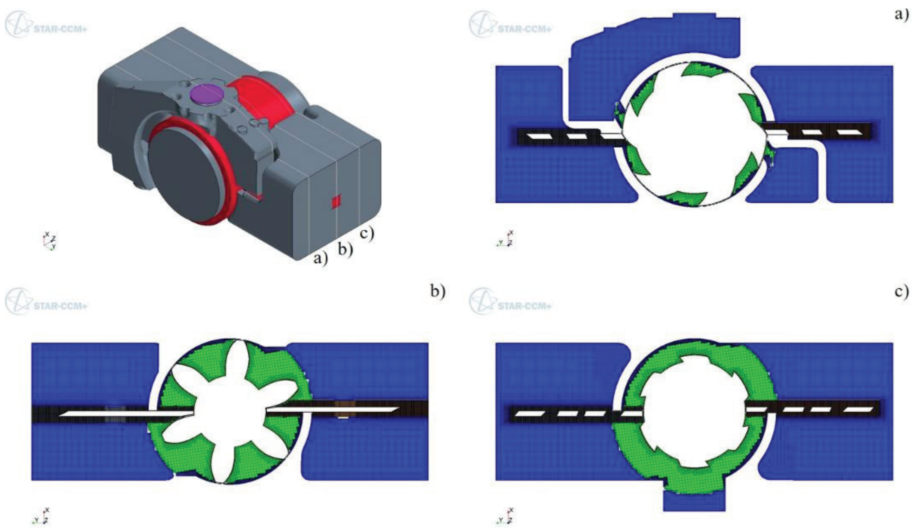

Fig. 3. Chimera geometry and planar section at a) inlet ports b) center of the device c) outlet port. It is possible to see the background region (blue) and the overlapping ones (yellow for the screw, grey and orange for the starwheels).

Cartesian elements and prism layer close to the wall.

As said before, the presence of three rotating regions implies the presence of three overset mesh boundaries. Moreover, as the gaterotor regions have to communicate between the background and the screw, the number of overset interfaces increases up to five (the three canonical between each rotating region and the background, and the two interfaces between the screw and the gaterotors). This number of interfaces is easily handled by the software, however it is possible that this could lead to higher solution time.

2.3. Mesh morphing

Metamorphosis (or Morphing) is the process of gradually changing a source object through intermediate objects into a target object [12]. Morphing a mesh to be used in a numerical simulation is a delicate task, especially for a 3D CFD mesh. The way the task is accomplished, depends on which smoothing algorithm is selected and on the definition of the control points criteria which can substantially change the result. The software in which mesh morphing is implemented and that is used in this paper is PumpLinx. This software has the capability of meshing pumps, gears and compressors by using this technique under the form of preloaded templates. In particular, the SCORG module has been designed for screw compressors. SCORG is a software for the design and analysis of screw compressors, pumps and rotors. The actual limit is given by the number of screw rotors that the SCORG module can deal with. In fact, only compressors with two or more screw rotors can be meshed with this template, which makes it unusable for a SSE application even if, the combination of structured mesh and prescribed motion, sounds to be the best approach to this kind of application.

3. Simulation analysis

The aforementioned meshing techniques have used to run simulations under steady-state conditions, with the exception of the CS one which was performed also under transient conditions. CS was the only meshing strategy that allowed the transient simulation to converge within the available computational resources and without numerical issues. The same boundary conditions have been applied to each simulation, i.e. an inlet pressure of 1200 kPa, an inlet temperature of 390 K, and an outlet pressure of 200 kPa. The chosen working fluid was air to simplify the analysis, and it as treated as an ideal gas. The standard turbulence model k-ε combined with standard wall functions were used. This model has proven to be the best compromise between accuracy, robustness and computational effort, as widely reported in open-literature.

The volumetric efficiency of the single screw expander, as well as other PD machines, is heavily affected by different kind of leakage paths [3]. A total of nine sealing lines can be identified in a single screw machines, as outlined in [4]. For instance, two gaps exist between the screw and satellite tooth tip and flank, the gap between satellite tooth tip and groove bottom (related to the manufacturing process, i.e. milling), the gap between housing and screw which allows the screw motion, the gaps between screw leading and trailing edges with the housing, the gap at the end curved edge of the groove, and tooth blowholes which existence is due to the imperfect shape of satellite teeth and the wear that occurs during operation. Both steady and transient simulations consider these leakage paths.

Regarding the computational mesh, different topologies have been used for the steady-state simulations. The PumpLinx General Mesher did not allow to set prism layers around the wall boundaries, while the meshes generated in STAR-CCM+ and Ansys Fluent did have the possibility to fully define the prism layers at the walls. Therefore, the hybrid mesh generated in STAR-CCM+ (Cartesian cells and prism layers) is made up of about 1,500,000 elements, the hybrid mesh generated in Ansys Fluent (tetrahedral cells and prism layers) is made up of about 3,000,000 elements while the Cartesian mesh generated in PumpLinx is made up of about 500,000 elements.

The transient simulation was performed only by means of the CS implemented in CD-ADAPCO STAR-CCM+ 10.02. Boundary conditions were kept the same, expect for the addition of the time step set to 10-4 s. The details of the mesh have been outlined in in the previous paragraph. The main rotor has a rotation speed of 3000 rpm, while the rotational speed of satellites have been obtained by considering the 6/11 engaging ratio between grooves and teeth.

4. Results

4.1. Steady state approach results

The results presented in the following are related to the C_d obtained in the three different simulations and are aimed at comparing the different approaches. The C_d is an index which, combined to the volumetric efficiency, can give information on the losses and on the leakage flows which occur in a positive displacement device. It is defined as follows:

$$C_d = \frac{Q}{A\sqrt{\frac{2\Delta p}{\rho}}} \qquad (1)$$

where Q is the volumetric flow rare [m^3/s], A is the passage area [m^2], Δp is the pressure drop [Pa] between two sections conveniently chosen upstream and downstream the passage area and ρ [kg/m^3] is the fluid density. The higher this value is, the higher are the losses due to leakage flow. To calculate this factor it is necessary to fix a section of known area A, across which the volumetric flux Q can be calculated by means of CFD simulations, and two arbitrary planes where it is possible to calculate the average pressure and, hence, the pressure drop. Figure 4 shows the section positions, referring to the simulation ran in STAR-CCM+. The calculations performed by means of the other methods rely on the same planes. The results are reported in Table 1. As can be seen, the C_d values for both Satellite 1 and Satellite 2 are of the same order of magnitude with a maximum difference of about 10%. Moreover, since Satellite 1 has a shorter duct, it was expected that the calculated C_d would be smaller than Satellite 2. The three calculations surprisingly predicted C_d values in close agreement each other (less than 1 % difference). In the case of Satellite 2, almost the same behaviour is noticed. The calculations predicted C_d values within a 5 % difference. This behaviour could have an explanation by considering that PumpLinx is optimized for transient

Table 1. Comparison between the Cd given by the steady simulations.

Software	C_d – Starwheel 1	C_d – Starwheel
Ansys Fluent 13.0	0.402	0.488
CD-ADAPCO STAR-CCM+ 10.02	0.402	0.497
PumpLinx 4.0.3	0.364	0.439

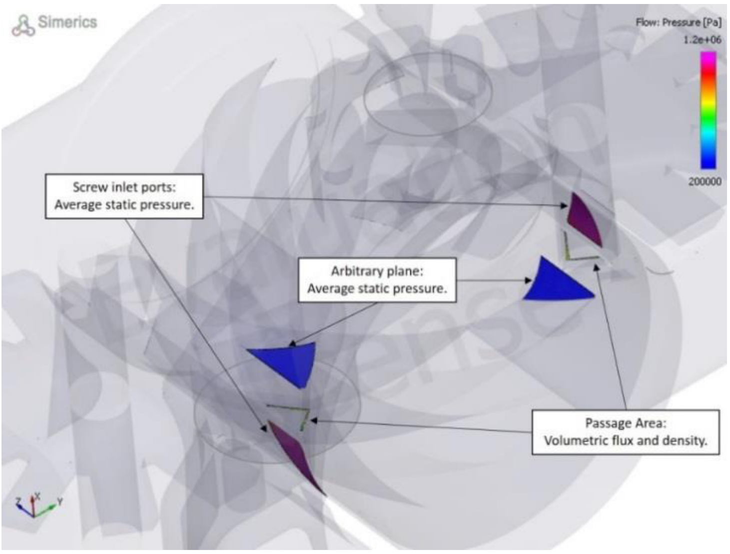

Fig. 4. Surfaces employed for the calculation of flow coefficients C_d.

calculations, and in particular the grid topology is conceived to meet this task. Nevertheless, also this software allowed the obtainment of C_d values which can be considered to achieve an enhanced information with respect to usual practice.

4.2. Transient approach results

A transient analysis provides insights on the dynamic behavior of the expander. As this work presents preliminary results of CFD simulations on a single-screw expander, particular attention is given to verify the reliability of the results obtained. In particular, the inlet and outlet pressure fluctuations are considered along with the torque generated at the main rotor shaft. Moreover, pressure fluctuations have also been monitored at the screw-expander triangular inlet port closest to the main inlet. The different variables of interest are plotted as a function of the normalized angular position of the screw. The mean values over one full rotation are then compared with the results obtained from the deterministic model [8]. In Figs. 5(a) and 5(b), it is possible to notice the three working chambers that are isolated by the gaterotors on the central screw. As expected, the gaterotors create three sections on the groove, lowering the pressure from the inlet to the discharge pocket. The contour of the pressure is overlaid on the main rotor. As shown in Fig. 6, the value of the shaft torque varies in the range from 65 Nm to 40 Nm, giving an output power of 16 kW (mean value). However, from the deterministic model, the maximum shaft power obtained was in the order of 9 kW. Similar values were also measured by running the expander with R245fa.

The pressure fluctuations at inlet and main rotor triangular ports are illustrated in Fig. 7. At the inlet port, the total pressure was imposed as boundary condition and the resulting fluctuations are clearly visible. The pressure fluctuations at the triangular inlet port present different trends suggesting that the inlet duct induces pressure waves and pressure drops. Such effects cannot be captured by the deterministic model without a coupling with a pressure pulsation model.

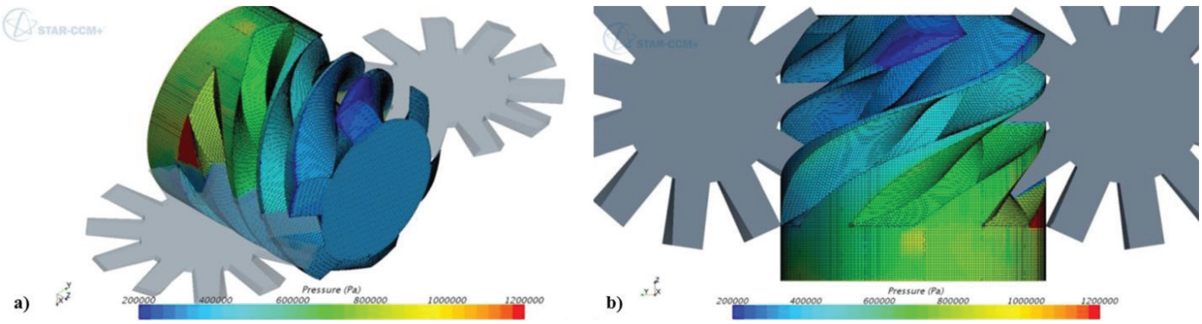

Fig. 5. Different working chambers (i.e. portion of the grooves) isolated by the gaterotors: (a) isometric view; (b) top view.

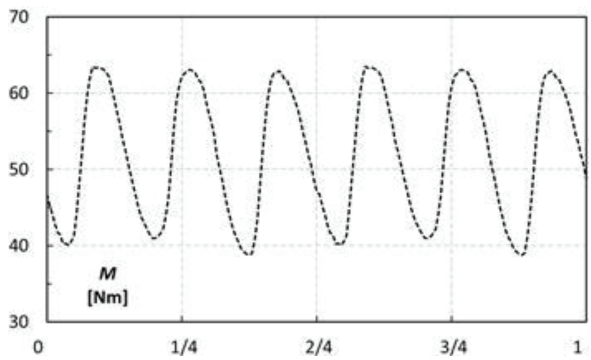

Fig. 6. Shaft torque (main screw rotor).

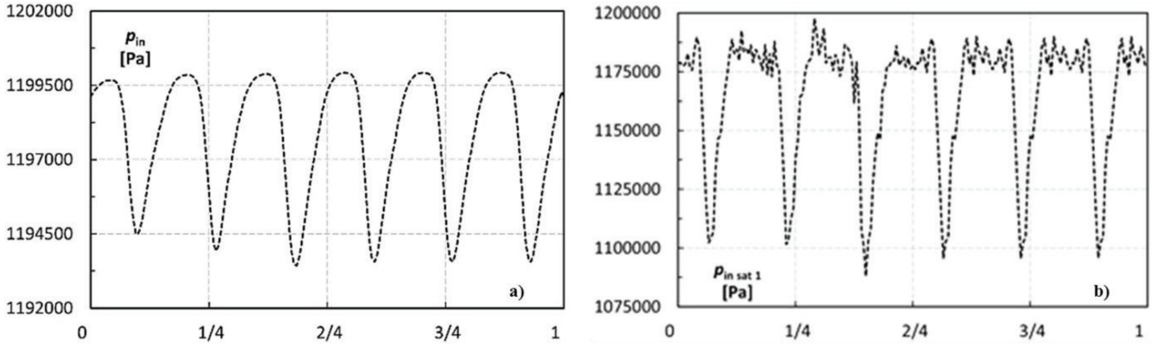

Fig. 7. Pressure at a) main inlet port and b) at the main rotor triangular port.

5. Conclusions

Different CFD approaches applied to a SSE are compared in this paper, both in steady-state and transient conditions. Different commercial software have been considered in order to identify the most suitable to simulate the SSE. All the evaluated software could perform a steady-state simulation to estimate the flow coefficients and a maximum deviation of 5 % was obtained, which can be considered acceptable. Regarding transient analysis, the fluid domain generated by the meshing of screw rotor and two starwheels makes the interpolation between overset and background regions critical and information is lost during the interpolation especially in regions such as gaps between screw and satellites. From the preliminary CFD results it can be concluded that CS showed some potential as meshing strategy for single screw type of machines. However, in order to improve the converge of the solution further work is required to investigate the influence of meshing parameters as well as the time-step taken.

References

[1] Quoilin, S., van den Broek, M., Declaye, S., Dewallef, P., Lemort, V., Techno-economic survey of Organic Rankine Cycle (ORC) systems. Renewable Sustainable Energy Rev 2013; 22:168-86.

[2] Imran, M., Usman, M., Park B-S, Lee, D.-H., Volumetric expander for low grade heat and waste heat recovery applications, Renewable Sustainable Energy Rev 2016, 57:1090-109.

[3] Ziviani, D., Bell, I., De Paepe, M., van den Broek, M., Comprehensive Model of a Single Screw Expander for ORC-Systems. Proc. of 22nd International Compressor Engineering Conference at Purdue, Purdue, 14 - 17 July, 2014, Paper n. 1506, pp. 1-10.

[4] Ziviani, D., Suman, A., Lecompte, S., De Paepe, M., van den Broek, M., Spina, P. R., Pinelli, M., Venturini, M., Beyene, A., Comparison of a Single-Screw and a Scroll Expander under Part-Load Conditions for Low-Grade Heat Recovery ORC Systems. Proc. of 6th International Conference on Applied Energy (ICAE2014), Taipei, 30 May - 2 June, 2014, Paper n. 78, pp. 1-4.

[5] Song, P., Wei, M., Shi, L., Danish, S. N., Ma, C., A review of scroll expanders for organic Rankine cycle systems. Appl. Therm. Eng. 2015, 75:54-64.

[6] Chang, J. C., Chang, C. W., Hung, T. C:, Lin, J. R., Huang, K. C., Experimental study and CFD approach for scroll type expander used in low-temperature organic Rankine cycle. Appl. Therm. Eng. 2014, 73:1444-52.

[7] Morini, M., Pavan, C., Pinelli, M., Romito, E., Suman, A., Analysis of a Scroll Machine for Micro ORC Applications by means of a RE/CFD Methodology. Appl. Therm. Eng. 2015, 80:132-40.

[8] Ziviani, D., Bell, I., De Paepe, M., van den Broek, M., Mechanistic model of an oil-flooded single-screw expander. Proc. of 23rd International Compressor Engineering Conference at Purdue, Purdue, 11 - 14 July, 2016, Paper n. 1486, pp. 1-10.

[9] Ziviani, D., Suman, A., Gabrielloni, J., Pinelli, M., De Paepe, M., van den Broek, M. CFD Approaches Applied to A Single-Screw Expander. Proc. of 23rd International Compressor Engineering Conference at Purdue, Purdue, 11 - 14 July, 2016, Paper n. 1488, pp. 1-10.

[10] Steger, J. L., Benek, J. A., On the use of composite grid schemes in computational aerodynamics, Comput. Methods Appl. Mech. Eng. 1987, 64:301–20. [11] Roget, B., Sitaraman, J., Robust and efficient overset grid assembly for partitioned unstructured meshes. J. Comput. Phys. 2014, 260:1-24.

[12] Lee A., Dobkin D., Sweldens W., Schroder P., Multiresolution Mesh Morphing. Proc. of SIGGRAPH 1999.